Supporting information for:

Activation of G-Protein-Coupled Receptors in Cell-Derived Plasma Membranes Supported on Porous Beads.

Sophie Roizard, [1] Christophe Danelon, [1†] Ghérici Hassaïne, [1] Joachim Piguet,[1]Katrin Schulze,[2] Ruud Hovius,[1] Robert Tampe[2] and Horst Vogel[1]*

[1]Laboratory of Physical Chemistry of Polymers and Membranes, Ecole Polytechnique Fédérale de Lausanne (EPFL), 1015 Lausanne, Switzerland; [2]Institute of Biochemistry, Biocenter, Center for Membrane Proteomics (CMP), Cluster of Excellence (CEF), Max-von-Laue-Str. 9, 60438 Frankfurt a.M., Germany; [†]Present address: Delft University of Technology, Kavli Institute of Nanoscience, Department of Bionanoscience, Lorentzweg 1, 2628 CJ Delft, The Netherlands.

SI0. Supplementary experimental section.

Reagents. Wheat-germ-agglutinin (WGA)-coated porous agarose beads, NECA (5′-N-ethyl-carboxamidoadenosine), XAC (1,3-dipropyl-8-phenylxanthine), and bovine calf serum were from Sigma. ZM241385 (4-(2-(7-amino-2-(2-furyl)-(1,2,4-triazolo[2,3](1,3,5-triazin-5-ylamino]ethyl)phenol) was from Tocris, ^{3}H-ZM241385 from American Radiolabeled Chemicals, HBSS (Hank's Buffered Salt Solution) and DMEM (Dulbecco's Modified Eagle Medium) from Invitrogen, APEC (2-[(2-aminoethylamino)-carbonylethylphenylethylamino]-5'-N-ethylcarboxamidoadenosine) from the National Institute of Health Chemical Synthesis and Drug Supply program. Tris-NTA conjugated to Atto647N8 or Atto565N8 were synthetized as described elsewhere[1]. Non-palmitoylated $G\alpha o_B$ carrying a His_6-tag at the N-terminus, and $G\beta\gamma$ from porcine cerebral cortex purified using a $G\alpha_{i1}$ affinity column were provided by Christoph Reinhart and Stephen Marino (Max Planck Institute of Biophysics in Frankfurt). $G\alpha o_B$ was stored at a concentration of 0.85 mM in a solution comprising 20 mM Tris-HCl pH 7.8, 100 mM NaCl, 5 mM $MgCl_2$, 5 mM DTT, 25 μM GDP. The $G\beta\gamma$ from porcine cerebral cortex was stored at a concentration of 1.6 mg/mL in 20 mM Hepes-KOH pH 7.4, 50 mM KCl, 0.1% $C_{12}E_9$, 10% glycerol. HEK293 TRex cells were provided by P.J. Reeves (Stony Brook University, NY).

Production of the stable cell line expressing A_{2A}R-Citrine. A stable cell line of HEK293 TRex was used carrying the plasmid pCDNA5-TO-A_{2A}R-mCitrine, which encodes the A_{2A}R fused with mCitrine (A_{2A}R-Citrine) at the C-terminus of the receptor. This cell line was obtained by PCR amplification and cloning of the cDNA of mCitrine into pSFVB-A_{2A}R[2] using Spe1 and Not1. The fusion A_{2A}R-YFP was amplified by PCR and cloned into pCDNA5-TO.

Expression of A_{2A}R-Citrine. HEK293 cells stably carrying the plasmid pCDNA5-TO-A_{2A}R-mCitrine were grown in DMEM containing 10% newborn calf serum. The heterologous expression of A_{2A}R-Citrine was induced upon addition of 2 μg/mL of tetracycline and 2 mM of Na-butyrate to the cell culture at 34°C. Before incubation

with beads, the cells were suspended 36 hours after induction and harvested in HBSS or PBS containing 1 mM EDTA.

HEK cells expressing pEYFP-ER or pEYFP-Golgi. The potential presence of fragments of endoplasmic reticulum (ER) and Golgi on cell membrane-coated beads was tested using HEK293 cells transfected with either EYFP-ER or EYFP-Golgi (two fusion proteins consisting of ER- or Golgi-targeting sequences and enhanced YFP; Clontech). Cells expressing EYFP-ER and EYFP-Golgi were collected 24 hours after transfection with Effectene (0.2 µg of DNA per well of a six-well plate). Plasma membrane-coated beads were prepared from these cells as described in the experimental section of the main article; the presence/absence of organelle fragments on the beads was investigated by confocal microscopy.

Synthesis of XAC-Atto655 and APEC-Atto633. XAC-Atto655 was synthesized from XAC (Sigma) and Atto655-NHS (Atto-tec) as described elsewhere[3]. The identity of the HPLC-purified product was confirmed by mass spectrometry (m/z = 938.6 ($M+H^+$)). APEC-Atto633 was synthesized by reacting 2-(4-(2-(2-aminoethylaminocarbonyl)ethyl)phenylethylamino)-5'-ethylcarboxyamidoadenosine-bis-trifluoroacetate (APEC-bis-trifluoroacetate, NIMH Chemical Synthesis and Drug Supply Program) with NHS-activated Atto655 (Atto-tec) [4]. The identity of the HPLC-purified product was confirmed by mass spectrometry (m/z = 1075.9 ($M+H^+$)).

Competitive binding data analysis. Considering that the ligand and the competitor bind reversibly to the same binding site, the binding of fluorescent ligand at equilibrium at the concentration of competitor [*L*] follows [5]:

$$F^L = a + \frac{(b-a)}{1+\frac{[L]}{IC_{50}}}.$$

F^L is the experimentally measured total fluorescence signal, *a* corresponds to the non-specific binding of labeled ligand and *b* is the maximal binding of labeled ligand in the absence of competitor.

The equation can be rewritten:

$$\frac{F^L - F^L_{NS}}{F^0 - F^0_{NS}} = \frac{1}{1+\frac{[L]}{IC_{50}}}.$$

F^L_{NS} is the fluorescence signal corresponding to non-specifically bound ligand, and F^0 and F^0_{NS} are the respective fluorescence signals corresponding to the total and non-specific bound ligand in absence of competitor. [*L*] is the free concentration of competitor which could be approximated by the total concentration of competitor added. Using the dissociation constants of the competitors ZM241385 and XAC, the amount of bound competitors were calculated to reach added maximally 8% of the total amount of competitors added.

The dissociation constant $K_D^{XACAtto655}$ of XAC-Atto655 was calculated according to the Cheng-Prusoff equation[6,7] using a value of the dissociation constant of ZM241385, K_i^{ZM} , reported in SI1:

$$K_i^{ZM} = \frac{IC_{50}^{ZM}}{1+\frac{[XACAtto655]}{K_D^{XACAtto665}}},$$

The dissociation constant K_i^{XAC} of XAC was calculated using the same relation:

$$K_i^{XAC} = \frac{IC_{50}^{XAC}}{1+\frac{[XACAtto655]}{K_D^{XACAtto665}}}.$$

Image acquisition. Micrographs of cells and beads were obtained using a laser scanning confocal microscope (ConfoCor LSM 510 META, Zeiss) equipped with a 40× objective (C Apochromat, water, NA 1.2, Zeiss). Conditions of excitation (exc) and emission (em): Citrine (exc 514 nm, em LP 530 nm), Atto565 (exc 561 nm, em BP 575-615 nm), Atto633, Atto647 and Atto655 (exc 633 nm, em LP 650). Detector gain, pinhole diameter and

laser power were kept constant for a given fluorescent probe enabling quantification of fluorescence intensities. The membrane-coated beads were transferred onto 0.16-mm thick glass coverslips and the experiments were performed at room temperature.

Image treatment. Four images representing the cross-sections of at least two beads were analyzed per sample. A procedure has been established to automate the analysis on the confocal cross-sections of the beads (Igor Pro, WaveMetrics). Basically, a binary mask was created for each image from the brightfield channel so that (i) the pixels along the bead cross-section perimeter were represented by digit 1, and (ii) the remaining pixels by digit 0. The mask obtained in this way was then multiplied to the corresponding intensity values of the fluorescence image. The average fluorescence along the bead cross-section was calculated for the several beads on each image.

The error bars depicted in the graphs correspond to the standard errors of the values of fluorescence intensities in between the eight images corresponding to each sample and its duplicate. Unless stated otherwise, scale bars correspond to 20 μm. For confocal microscope images depicted in the article and supplementary information a gamma correction of 0.63 has been applied to the images before representation (imageJ).

The surface area of the beads covered with membranes was determined using 3D reconstituted images. These images were obtained after deconvolution of a z-stack of confocal images using HuygensPro software (Scientific Volume Imaging). A threshold value was set to discriminate between background signal and Citrine fluorescence on the bead. The percentage of the bead's surface area covered by membranes was calculated as the number of pixels having fluorescence intensities above the threshold divided by the total number of pixels of the bead surface area. This analysis was performed on five different beads obtained from three different bead batches leading to a mean value of 80 ± 5 % of the bead surface area covered with membranes.

SI1. Determination of the number of A_{2A}Rs per cell.

The average number of receptors expressed per cell was obtained by determining the number of bound ligands ^{3}H-ZM241385 to the plasma membrane of whole cells. Cells were grown and A_{2A}R expression was induced as described (SI0). 36 hours after induction, the cells were gently harvested, centrifuged (1200 rpm, 4 min, 4°C) and resuspended in Hepes 10 mM to obtain a concentration of 1×10^6 cells/mL. ^{3}H-ZM241385 binding to the cells was carried out in triplicates by incubating 1 mL samples (5×10^4 cells/mL) for 90 minutes at room temperature at ligand concentrations ranging from 0.1 to 30 nM. Non-specific binding was determined in the presence of 30 μM non-radioactive ZM241385.

Specific binding of ligand to the receptor was determined by fitting the concentration of ligand-receptor complexes [*RL*] as a function of the initial concentration of ^{3}H-ZM241385 (Fig. SI1) by a Langmuir isotherm taking into account the ligand depletion in the bulk solution and the standard deviation of each triplicated data point, according to:

$$[RL] = \frac{(K_D + [R_0] + [L_0]) - \sqrt{(K_D + [R_0] + [L_0])^2 - 4[R_0]\times[L_0]}}{2},$$

where $[R_0]$ is the initial concentration of receptors, $[L_0]$ the initial concentration of ^{3}H-ZM241385 and K_D the dissociation constant. The calculated values of K_D = 0.24 ± 0.08 nM and $[R_0]$ = 0.28 ± 0.04 nM (χ^2= 0.47) are in agreement with the K_D value published elsewhere[8]. Considering the number of cells per assay each cell comprises on average 3.4 ± 0.5×10^6 A_{2A}Rs, which corresponds to 1.5 ×10^3 A_{2A}R-Citrine/μm^2 considering the surface of a swollen HEK cell to be 2300 μm^2.[9]

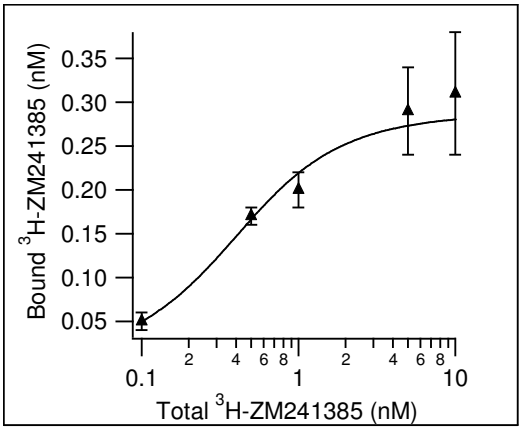

Figure SI1. Binding of ^{3}H-ZM241385 to HEK293 cells expressing A_{2A}R-Citrine.

SI2. Ligand binding to A_{2A}R.

Ligand binding to beads coated with membranes, which either contain or are devoid of A_{2A}R-Citrine resulted in the appearance of a fluorescence signal at the surface of the bead (Fig. SI2). However, in the presence of A_{2A}R-Citrine the binding was significantly higher demonstrating specific interaction between the GPCR and the ligands. Non-specific binding ranged between 20 to 30% of total binding (Fig. SI2).

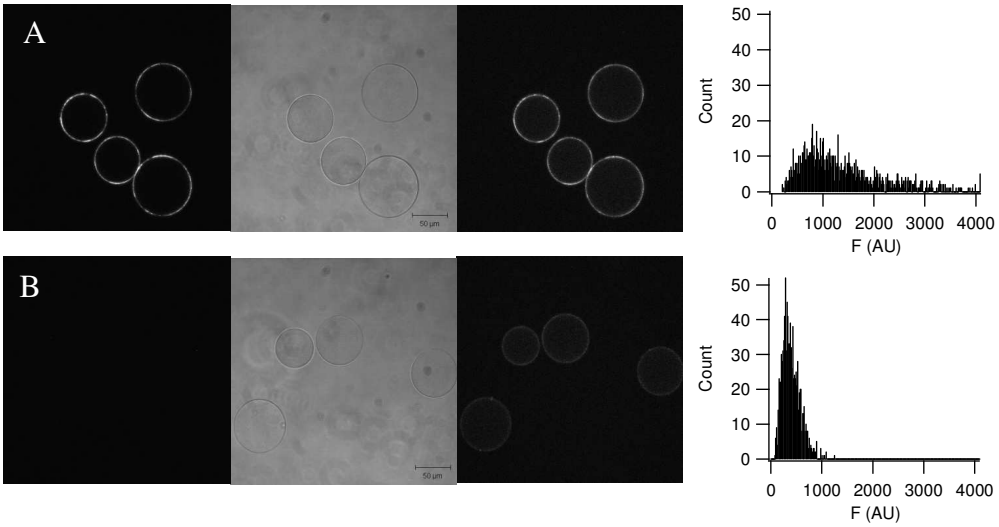

Figure SI2. Ligand binding to A_{2A}R on beads. (A) Confocal fluorescence micrograph of beads coated with cell membranes comprising A_{2A}R-Citrine after two hours of incubation with 40 nM of APEC-Atto633. From left to right: citrine fluorescence, transmission image, Atto633 fluorescence. The histogram represents the intensity distribution of fluorescence of APEC-Atto633 of the pixels at the rim of the beads. The average normalized fluorescence intensity on the surface of the beads is 1373. (B) As (A) but using beads coated with cell membranes devoid of A_{2A}R. The average normalized fluorescence intensity on the surface of the beads is 408.

SI3. G protein binding to $A_{2A}R$.

SI3.1. Assembly of the fluorescent heterotrimeric G proteins

G proteins were reconstituted using purified His_6-Gα, purified Gβγ complexes containing their native membrane anchor and the fluorescent probe Tris-NTA-Pro8-Atto647N[1] (hereafter named Atto647) which binds selectively with high affinity to the hexahistidine sequence of Gα. The three components were incubated in relative proportions of Atto647:Gα:Gβγ = 0.75:1:2 in TNMEB buffer together with 2 μM GDP for 1 h on ice prior adding to the membrane-covered beads. Several species could form in solution such as Gα-βγ, Gαβγ-Atto647, and Gα-Atto647. The concentrations of the different G protein species in solution for each initial set of concentrations {[Atto647], [Gα], [Gβγ]} were calculated considering that (i) the association of Gβγ to Gα is independent of the presence of Atto647 on Gα, and (ii) the binding of Atto647 dye to Gα and Gα-βγ is identical. The biochemical system could thus be described as follows:

$$G_\alpha + G_{\beta\gamma} \leftrightarrow G_{\alpha\beta\gamma} \quad (1)$$

$$Atto647G_\alpha + G_{\beta\gamma} \leftrightarrow Atto647G_{\alpha\beta\gamma} \quad (2)$$

(1) and (2) have the same dissociation constant $K_{D1} = 2.9\times10^{-9} M$ [10].

$$G_\alpha + Atto647 \leftrightarrow Atto647G_\alpha \quad (3)$$

$$G_{\alpha\beta\gamma} + Atto647 \leftrightarrow Atto647G_{\alpha\beta\gamma} \quad (4)$$

(3) and (4) have the same dissociation constant $K_{D2} = 2.1\times10^{-9} M$ [11].

The preparation of fluorescent Atto647-Gα was carried out similarly after mixing of Atto647 and purified Gα in a 0.75:1 ratio. The concentrations of Atto647-Gα and unlabeled Gα in solution for each initial set of concentrations of {[Atto647], [Gα]} were calculated considering the dissociation constant K_{D1}.

SI3.2. Determination of the dissociation constant K_D of Gαβγ-$A_{2A}R$ complex

To assess the dissociation constant K_D of the complex between Gαβγ and $A_{2A}R$ we assumed that (i) the depletion of G proteins upon binding to the receptors was negligible, (ii) the labeling with Atto647 did neither affect the interaction between Gα and Gβγ, nor between Gαβγ and $A_{2A}R$. However, the presence of unlabeled Gαβγ complexes in the solution had to be taken into account because the relative proportion of unlabeled versus labeled Gαβγ complexes depends on the total concentration of each component. Total binding of (fluorescent and non-fluorescent) G proteins at each particular condition was estimated from the fluorescence signal of bound Atto647-Gαβγ assuming that the binding of unlabeled and Atto647-labeled Gαβγ to the receptors is identical. This is reasonable since binding of G protein to the receptor occurs at the C-terminal part of Gα, whereas the Atto647 dye was attached to the N-terminus of Gα. Therefore the total amount of bound Atto647-Gαβγ could be extracted from the fluorescence signal of bound Atto647-Gαβγ and the ratio of free Atto647-G proteins over free unlabeled G proteins.

SI3.3. Total and non-specific binding of Gα-Atto647 and Gαβγ-Atto647 to cell membrane-coated beads.

Fluorescent heterotrimeric G proteins composed of Atto647-Gαβγ bound to cell membrane-coated beads, which either contain or are devoid of A_{2A}R-Citrine. However, in the presence of A_{2A}R-Citrine the binding of G proteins was significantly higher demonstrating specific interaction between the GPCR and the G protein. Interestingly, Gα alone was not able to bind to the receptors.

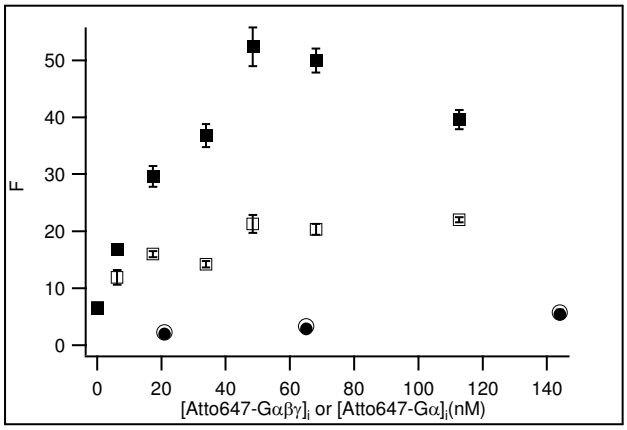

Figure SI3.3. Binding of Gα-Atto647 (circles) and Gαβγ-Atto647 (squares) to cell membrane-coated beads, which contain (•, ■) or are devoid of (○, □) A_{2A}R-Citrine.

SI4. Inside-out tethering of native membranes on lectin-coated beads.

Our method of transferring plasma membrane sheets from live cells to WGA-coated beads yielded a well-defined inside-out membrane orientation because cells attached specifically to WGA on the beads via their extracellular glycosylated leaflet on the plasma membrane. We prove this orientation as follows: when cells in suspension are first incubated with soluble WGA and then incubated with WGA-coated beads, they do not attach to the beads (Fig. SI4).

Experimental details. HEK 293 cells stably expressing the neurokinin-1 receptor fused with the Green Fluorescent Protein at the C-terminus (NK_1R-GFP) were grown for 48 h in DMEM containing 10% newborn calf serum. The cells were suspended and harvested in PBS containing 1 mM EDTA. One half of the cell culture in suspension was then incubated with WGA at a final concentration of 15 mg/mL at 4°C for 20 minutes, the other half was kept on ice. The subsequent procedure to prepare membrane-coated beads was carried-out as described in the main text of the article using the two batches of cells in parallel.

The two batches of cells mixed with beads were investigated by confocal microscopy before and after cell disruption (Fig. SI4). When WGA was added in solution to the cells it blocked the glycosylation sites on the cell surfaces preventing the subsequent attachment of whole cells to WGA-coated beads (Fig. SI4 B compared to SI4 A); after cell disruption, no plasma membrane patches bind non-specifically to the WGA-coated beads (Fig. SI4 D).

In conclusion, the method presented here transfers native membrane sheets on beads in an inside-out orientation by selective and high-affinity binding of the glycosylated extracellular plasma membrane surface.

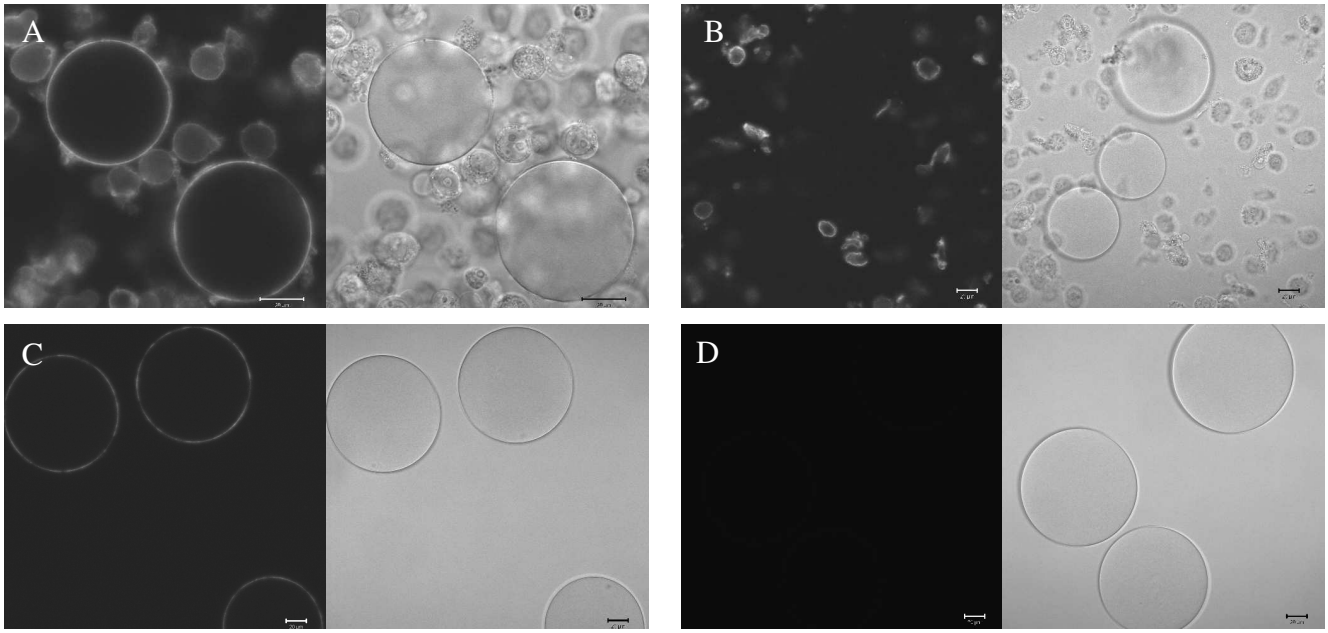

Figure SI4. Confocal fluorescence micrographs showing beads mixed with HEK293 cells expressing the NK_1R-GFP (A). For (B) the cells have been pre-incubated with WGA. The fluorescence results from NK_1R-GFP expressed at the cell plasma membrane. Image A shows that whole cells bind to WGA-coated beads and detach leaving plasma membrane sheets on the surface of the beads. B shows that cells do not bind to WGA-coated beads after incubation with soluble WGA. Most of the cells in B appear non-fluorescent because they are sitting on the coverslip out of the focal plane. (C, D) Native membrane-coated beads obtained from the samples (A) and (B) after cell disruption and wash. The fluorescence at the circumference of the beads on (C) results from NK_1R-GFP of cell plasma membranes coating the beads. Such fluorescence is not detectable on (D) demonstrating the absence of plasma membrane sheets tethered on the surface of the beads. In each of the four panels the fluorescence image is depicted on the left and the corresponding transmission image on the right hand side.

SI5. Specific ligand binding to other transmembrane receptors.

To demonstrate the generic potential of our method for other transmembrane receptors we used WGA-coated beads covered with native membranes containing (i) a GPCR, the neurokinin 1 receptor fused with GFP (NK_1R-GFP), and (ii) a serotonin gated ionotropic receptor, the 5-HT_3R. In both cases, binding of fluorescent ligands could be observed at the rim of the beads and could be displaced by an excess of unlabeled competitor (Fig. SI5). Such specific ligand binding demonstrates the presence of the transmembrane proteins on the membrane-coated beads with a preserved accessibility and functionality of their ligand binding sites.

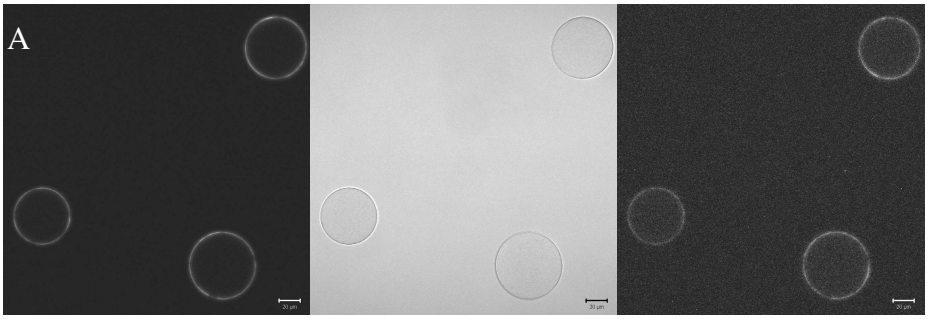

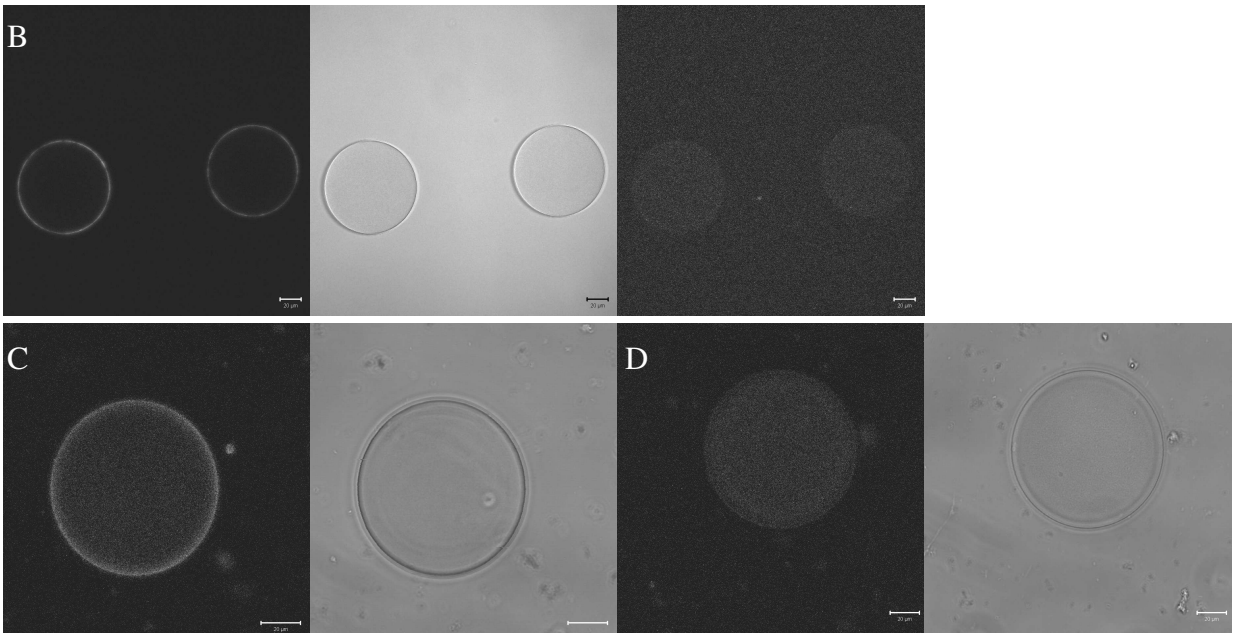

Figure SI5. (A, B) Binding of 25 nM substance-P-Cy5 (a NK_1R-specific agonist [12]) to membrane-coated beads containing NK_1R-GFP in the absence (A) or in the presence of 1.3 μM of unlabelled substance P (B). From left to right: fluorescence of NK_1R-GFP at surface of beads, transmission image, fluorescence of substance-P-Cy5. Binding of substance-P-Cy5 is prevented in the presence of non-fluorescent competitor as shown in row B compared to A. (C, D) Binding of GR-fluorescein (a $5HT_3R$-specific ligand [13]) to membrane-coated beads containing 5-HT_3R in the absence (C) or in the presence of 1 μM of the competing ligand quipazin (D). Left: fluorescence of GR-fluorescein; right: transmission image. Binding of GR-fluorescein is prevented in the presence of non-fluorescent competitor quipazine as shown on picture D compared to C.

SI6. Complete references 9, 21, 43, 64

(9) Rasmussen, S. G.; Devree, B. T.; Zou, Y.; Kruse, A. C.; Chung, K. Y.; Kobilka, T. S.; Thian, F. S.; Chae, P. S.; Pardon, E.; Calinski, D.; Mathiesen, J. M.; Shah, S. T.; Lyons, J. A.; Caffrey, M.; Gellman, S. H.; Steyaert, J.; Skiniotis, G.; Weis, W. I.; Sunahara, R. K.; Kobilka, B. K. *Nature* **2011**.

(21) Schroder, R.; Janssen, N.; Schmidt, J.; Kebig, A.; Merten, N.; Hennen, S.; Muller, A.; Blattermann, S.; Mohr-Andra, M.; Zahn, S.; Wenzel, J.; Smith, N. J.; Gomeza, J.; Drewke, C.; Milligan, G.; Mohr, K.; Kostenis, E. *Nat Biotech*, **2010**, 28, 943-949.

(43) Knoll, W.; Bender, K.; Farch, R.; Frank, C.; Gatz, H.; Heibel, C.; Jenkins, T.; Jonas, U.; Kibrom, A.; Kagler, R.; Naumann, C.; Naumann, R.; Reisinger, A.; Rahe, J.; Schiller, S.; Sinner, E.-K.; Meier, W. P.; Springer Berlin /Heidelberg: **2010**; Vol. 224, p 87-111.

(64) Lee, Y.-C.; Block, G.; Chen, H.; Folch-Puy, E.; Foronjy, R.; Jalili, R.; Jendresen, C. B.; Kimura, M.; Kraft, E.; Lindemose, S.; Lu, J.; McLain, T.; Nutt, L.; Ramon-Garcia, S.; Smith, J.; Spivak, A.; Wang, M. L.; Zanic, M.; Lin, S.-H. *Protein Express Purifi* **2008**, *62*, 223-229.

SI7. Supporting Information References

(1) Grunwald, C.; Schulze, K.; Giannone, G.; Cognet, L.; Lounis, B.; Choquet, D.; Tampe, R. *J Am Chem Soc* **2011**, *133*, 8090-8093.

(2) Hassaine, G.; Wagner, R.; Kempf, J.; Cherouati, N.; Hassaine, N.; Prual, C.; André, N.; Reinhart, C.; Pattus, F.; Lundstrom, K. *Protein Expr Purif* **2006**, *45*, 343-351.

(3) Briddon, S. J.; Middleton, R. J.; Cordeaux, Y.; Flavin, F. M.; Weinstein, J. A.; George, M. W.; Kellam, B.; Hill, S. J.; Black, J. W. *Proc Natl Acad Sci U S A* **2004**, *101*, 4673-4678.

(4) Brand, F.; Klutz, A. M.; Jacobson, K. A.; Fredholm, B. B.; Schulte, G. *Eur J Pharmacol.* **2008**, *590*, 36-42.

(5) *Fitting Models to Biological Data Using Linear and Nonlinear Regression. A pratical guide to curve fitting*; Motulsky, H.; Christopoulos, A., Eds.; Oxford University Press, **2004**.

(6) Cheng, Y.; Prusoff, W. H. *Biochem Pharmacol* **1973**, *22*, 3099-3108.

(7) *Drug-Acceptor Interactions*; Bindslev, N., Ed.; Co-Action Publishing, **2008**.

(8) Alexander, S. P. H.; Mathie, A.; Peters, J. A. *Br J Pharmacol* **2007**, *150*, S1-S1.

(9) Pick, H.; Preuss, A. K.; Mayer, M.; Wohland, T.; Hovius, R.; Vogel, H. *Biochemistry* **2003**, *42*, 877-884.

(10) Sarvazyan, N. A.; Remmers, A. E.; Neubig, R. R. *J Biol Chem* **1998**, *273*, 7934-7940.

(11) Lata, S.; Reichel, A.; Brock, R.; Tampe, R.; Piehler, J. *J Am Chem Soc* **2005**, *127*, 10205-10215.

(12) Meyer, B. H.; Martinez, K. L.; Segura, J.-M.; Pascoal, P.; Hovius, R.; George, N.; Johnsson, K.; Vogel, H. *FEBS Letters* **2006**, *580*, 1654-1658.

(13) Tairi, A. P.; Hovius, R.; Pick, H.; Blasey, H.; Bernard, A.; Surprenant, A.; Lundstrom, K.; Vogel, H. *Biochemistry* **1998**, *37*, 15850-15864.

(14) Rasmussen, S. G.; Devree, B. T.; Zou, Y.; Kruse, A. C.; Chung, K. Y.; Kobilka, T. S.; Thian, F. S.; Chae, P. S.; Pardon, E.; Calinski, D.; Mathiesen, J. M.; Shah, S. T.; Lyons, J. A.; Caffrey, M.; Gellman, S. H.; Steyaert, J.; Skiniotis, G.; Weis, W. I.; Sunahara, R. K.; Kobilka, B. K. *Nature* **2011**.